ISSN 0304-9892 (Print) ISSN 2455-7463 (Online)
www.vijnanaparishadofindia.org/jnanabha

Jñānābha, **Vol. 55(2) (2025), 67-82**

A MATHEMATICAL MODELLING STUDY FOR DESALINATION OF SEA-WATER USING MARSH PLANTS

Deepika Marwar[1], Alok Malviya[2], Maninder Singh Arora[3]
[1,2]Department of Mathematics, VSSD(PG) College, CSJM University, Kanpur, Uttar Pradesh, India-208002
[3]Department of Mathematics, PPN (PG) College, CSJM University, Kanpur, Uttar Pradesh, India-208001
Email: deepika91marwar@gmail.com, alok92nov@gmail.com, manindersingharora_kn04@csjmu.ac.in
(Received: August 02*,* 2025*, In format: September* 01*,* 2025*; Revised: October* 02*,* 2025*; Accepted: October* 04*,* 2025*)*

DOI: https://doi.org/10.58250/jnanabha.2025.55209

Abstract

Water scarcity poses a significant challenge, particularly in regions affected by drought or inherently dry conditions, leading to a stark imbalance between the availability and demand for fresh water. This situation underscores the necessity for water conservation, purification for reuse, and desalination. Among the various strategies employed for desalination, utilizing marsh plants is one of the most cost-effective approaches. This paper focuses on enhancing the availability of potable water through economical methods, specifically the use of marsh plants within water reservoirs. We introduce a nonlinear mathematical model to examine the process of desalinating saline water in a reservoir environment, considering the interplay between soil properties and marsh plants growth, which is influenced by the salinity levels in both water and soil. Our study involves four nonlinearly interacting variables: salt concentration in the water, biomass density of marsh plants, soil concentration, and salt concentration in the soil. We have established the existence of an equilibrium point through isocline analysis. The analytical exploration of the model includes determining the local and global stability of the equilibria. The validity of our findings is further corroborated through numerical simulations for graphical representations and sensitivity analysis of the system with respect to key parameters.
2020 Mathematical Sciences Classification: 34D20, 34D23, 34A34.
Keywords and Phrases: Desalination, Marsh plants, Soil salinization, Sensitivity.

1 Introduction

Over the past century, the demand for freshwater has surged on a global scale, and this trend shows no signs of slowing down, with an annual growth rate of approximately 1% [23]. The projections from the Water Resource Group 2030 indicate that by 2030, the world's population will grapple with a staggering 40% deficit in potable water[13]. At least 1.7 billion people consume contaminated water in water-stressed countries and face water-borne diseases like diarrhoea, cholera, dysentery, etc [18]. Industrial development and various other economic activities heavily rely (approximately 75%) on a sustainable water supply. Sustainable water management in mining industries reduces freshwater use through recycling and efficient practices, helping to ease existing water scarcity [17]. Shockingly, projections by the World Bank suggest that by 2050, *GDP* in water-stressed regions could plummet by 6% due to the adverse impacts of water scarcity on health, income, and agricultural production [3].

The majority of Earth's water resources are saline, rendering them unsuitable for agricultural use and other purposes, thereby hampering agricultural productivity [22]. Given that, nearly 97.5% of the world's total water exists in oceans as saline water, desalination emerges as a pivotal solution to alleviate water stress [8]. Desalination, the process of obtaining pure, potable water by removing salt and impurities from available water sources, is facilitated by various technologies globally, including reverse osmosis, multi-effect-distillation, and multi-stage flash desalination plants [5]. With approximately 19,744 desalination plants worldwide having a capacity of 99.7 million m^3 per day production, they cater to the needs of over 300 million people across 150 countries [2, 25].

However, the desalination process poses environmental challenges, including marine pollution from brine extraction, groundwater contamination, noise pollution, air pollution, and energy loss [7]. To mitigate these

adverse impacts, the adoption of greener desalination approaches such as gas hydrate-based desalination and the utilization of renewable energy sources like geothermal energy, solar water evaporation desalination and hybrid desalination systems is imperative [6, 11, 12]. It is crucial to prioritize technologies that yield water with low salinity, minimal environmental footprint, and optimal operational costs [28]. Policymakers' focus in the current landscape is on attaining fresh water through cost-effective and environmentally friendly desalination processes, with a notable emphasis on leveraging natural solutions like marsh plants and salt-tolerant organisms, which offer cost-effective alternatives already present in nature [1, 21]. Marsh plants exhibit robust growth in response to salinity levels of up to 200 mol/m^3, demonstrating remarkable tolerance to high salinity conditions [20].

Furthermore, numerous studies have explored aerobic and anaerobic environments for the biological treatment of saline water [4, 14, 15, 19, 24, 26, 27]. A non-linear mathematical model has been proposed to remove the inorganic pollutants from the water body by the biosorption procedure using fungal inhabitants [9]. Using the concept of prey-predator modelling, Shukla *et al.* [21] have proposed a mathematical model in which marsh plant and halophile bacteria have been considered as predators and saline water as prey for the desalination process via Michaelis Menten kinetics [21]. Goyal *et al.* [9] have also proposed and analyzed a predator-prey model system for desalinization as well as the removal of pollutants from the water using halophiles [10].

In light of escalating global population growth and the pressing water crisis, this study introduces a novel non-linear mathematical model for desalination. Specifically, we integrate soil factors to simulate the growth of marsh plants in reservoirs containing saline water, a concept hitherto unexplored in existing literature. The growth of marsh plants depends upon the concentration of salt in water. The proposed model accounts for soil salinization dynamics, where both marsh plants and soil absorb salt from water, thereby reducing its salinity. By using this innovative approach, optimal results for desalination can be achieved in a cost-effective and environmentally sustainable manner, devoid of adverse ecological impacts.

1.1 Comparison with Previous Models

Several researchers have previously employed mathematical modelling techniques to investigate the potential of halophytes and halophytic plants as natural systems for desalinating saline water. In contrast, our proposed model uniquely captures not only the role of halophytic marsh plants in the desalination process but also treats soil salinity as a dynamic variable, offering a novel perspective on the systems behavior. Below, we compare our work with key previous studies:

1. Shukla *et al.* [21] proposed a nonlinear mathematical model in which marsh plants and halophiles were treated as predators and saline water as prey. However, their study concentrated primarily on desalination and did not account for the role of soil or the dynamics of soil salinity [21].
2. Ashish Goyal *et al.* [9] developed a nonlinear mathematical model that explores the removal of inorganic pollutants from water through the bio-absorption process mediated by fungi [9].
3. Ashish Goyal *et al.* [10] proposed a two-prey, one-predator model in which halophiles play a central role in reducing both salinity and pollutants [10].
4. Our study builds upon earlier work by incorporating soil dynamics, which not only aid in reducing salt content from water but also support the growth of marsh plants. Distinct from previous models, we focus exclusively on halophytic marsh plants while considering soil salinity as a mediating factor in the desalination of saline water.

2 Model Formulation

To formulate the model for the desalination of saline water using marsh plants in a reservoir, we consider four non-linearly interacting variables listed as follows:

(i.) The concentration of salt in water at time t denoted by $s(t)$ (in g/L),
(ii.) The biomass density of marsh plants at time t denoted by $M(t)$ (in g per square m),
(iii.) The concentration of soil in the reservoir at time t denoted by $S(t)$ (in kg/L), and
(iv.) The concentration of salt in soil due to soil salinization at time t denoted by $s_c(t)$ (in mg/L).

Here, we consider the desalination of saline water within a reservoir containing soil and marsh plants. Both marsh plants and soil extract the salt from the saline water. We assume that the rate of growth for the concentration of salt in water is proportional to the difference of its equilibrium concentration s_0 and its concentration s at time t that is $(s_0 - s)$ and marsh plants take the salt from saline water for its growth,

so β_1 is the depletion rate coefficient for the salt concentration due to salt extraction for growth of marsh plants. Now, the depletion rate of salt from seawater due to absorption by soil is denoted by β_2. Thus, the dynamics of concentration of salt in water is given by the following differential equation:

$$\frac{ds}{dt} = \beta(s_0 - s) - \beta_1 sM - \beta_2 sS.$$

We assume that the growth of marsh plants follows the logistic model with intrinsic growth rate coefficient γ and γ_0 represents its natural depletion. The plant growth equation incorporates both direct growth and salt-mediated contributions. This reflects the behaviour of halophytic marsh plants, which are known to tolerate and even thrive under moderate-to-high salinity levels [20]. Hence, the growth rate of marsh plants in the reservoir is given by the following differential equation:

$$\frac{dM}{dt} = \gamma(M - \frac{M^2}{K}) - \gamma_0 M + \gamma_1\beta_1 sM + \gamma_2\theta_1 s_c M.$$

Here, γ_1 and γ_2 both are proportionality constants, $0 < \gamma_1, \gamma_2 < 1$. The terms involving $\gamma_1\beta_1 sM$ and $\gamma_2\theta_1 s_c M$ represent the positive influence of dissolved and soil-bound salts within the physiologically relevant salinity range. Although at very high concentrations salinity becomes inhibitory, Our model aims to capture the initial positive response typical of halophytes, making them suitable candidates for cost-effective desalination. In the present model, $S(t)$ is interpreted not as the entire soil mass but as the effective concentration of active soil sites or suspended particles that participate in salt absorption. Now, we assume that the rate of growth of soil concentration is directly proportional to the difference of its equilibrium concentration S_0 and its concentration S at time t with growth rate coefficient δ and a decrease in $S(t)$ represents the temporary reduction in the effective availability of absorption sites under salinity stress, rather than literal soil depletion with its depletion rate coefficient β_2. Now, the rate of change of soil concentration is given by the differential equation:

$$\frac{dS}{dt} = \delta(S_0 - S) - \beta_2 sS.$$

Here, The interaction term $\beta_2 sS$ therefore, captures the finite salt-buffering capacity of soil. The replenishment term $\delta(S_0 - S)$ accounts for natural processes such as leaching, sediment turnover, and microbial action that restore soil buffering capacity over time. This abstraction allows us to highlight the essential role of soil as a dynamic regulator in the desalination process.

Let us assume that the rate of growth of concentration of salt in the soil is equal to the amount of soil obtained after soil-buffering capacity of soil, that is $\theta\beta_2 sS$, where θ is the proportionality constant $0 < \theta < 1$. Also, the concentration of salt in the soil depletes naturally due to leaching, climate, some microorganism and fungi etc [16]. The natural depletion coefficient is θ_0 and depletion due to marsh plant consumption is $\theta_1 s_c M$, where θ_1 is depletion rate coefficient due to M. Thus, we get the following differential equation:

$$\frac{ds_c}{dt} = \theta\beta_2 sS - \theta_0 s_c - \theta_1 s_c M.$$

Now, combining the above four equations, the system showing interrelation of four variables is depicted in Figure 2.1 and the model system for desalination is as follows:

$$\left.\begin{aligned} \frac{ds}{dt} &= \beta(s_0 - s) - \beta_1 sM - \beta_2 sS, \\ \frac{dM}{dt} &= \gamma(M - \frac{M^2}{K}) - \gamma_0 M + \gamma_1\beta_1 sM + \gamma_2\theta_1 s_c M, \\ \frac{dS}{dt} &= \delta(S_0 - S) - \beta_2 sS, \\ \frac{ds_c}{dt} &= \theta\beta_2 sS - \theta_0 s_c - \theta_1 s_c M, \end{aligned}\right\} \tag{2.1}$$

where, $s(0) \geq 0$, $M(0) \geq 0$, $S(0) \geq 0$, $s_c(0) \geq 0$. All the parameters are taken to be positive for the system.

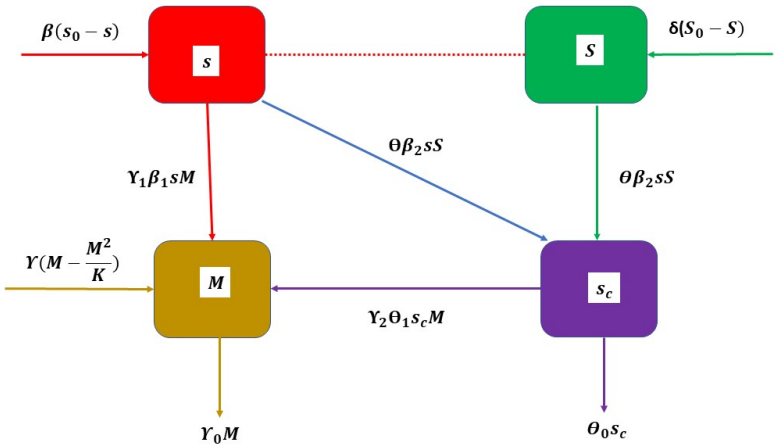

***Figure* 2.1:** *Schematic representation of interrelation among variables*

3 Bounds of variable

Variables of the system (2.1) remain bounded inside the region of attraction. The following lemma defines the region of attraction and provides the bounds of variables.

Lemma 3.1. *The set* $\Gamma=\{(s,M,S,\ s_c)\in R_+^4:\ 0 \le s \le s_{max},\ 0 \le M \le M_{max},\ 0 \le S \le S_{max},\ 0 \le s_c \le s_{c_{max}}\}$,

where, $s_{max} = s_0,\ M_{max} = \dfrac{[\gamma - \gamma_0 + \gamma_1\beta_1 s_0 + \gamma_2\theta_1 s_{c_{max}}]K}{\gamma},\ S_{max} = S_0,\ s_{c_{max}} = \dfrac{\theta\beta_2 s_0 S_0}{\theta_0}$ *represents the region of attraction for the dynamical system* (2.1) *which brings inside all solutions starting in the interior of the positive orthant.*

Proof. From first equation of the system (2.1) we get,

$\dfrac{ds}{dt} \le \beta(s_0 - s)$

$\Longrightarrow \lim\limits_{t\to\infty} sups(t) \le s_0 = s_{max}$ (say).

Again, from second equation we obtain,

$\dfrac{dM}{dt} \le \gamma M(1 - \dfrac{M}{K}) - \gamma_0 M + \gamma_1\beta_1 sM + \gamma_2\theta_1 s_c M$

$\Longrightarrow \lim\limits_{t\to\infty} supM(t) \le K\dfrac{\gamma - \gamma_0 + \gamma_1\beta_1 s + \gamma_2\theta_1 s_c}{\gamma} = M_{max}$ (say).

Further, from the third equation, we get

$\dfrac{dS}{dt} \le \delta(S_0 - S)$

$\Longrightarrow \lim\limits_{t\to\infty} supS(t) \le S_0 = S_{max}$ (say).

Now, from the fourth equation, we get

$\dfrac{ds_c}{dt} \le \theta\beta_2 sS - \theta_0 s_c$

$\Longrightarrow \lim\limits_{t\to\infty} sups_c(t) \le \dfrac{\theta\beta_2 s_0 S_0}{\theta_0} = s_{c_{max}}$ (say).

Hence, the proof. □

4 Equilibrium Analysis

In this section, we analyze the proposed non-linear system (2.1). The equilibrium point of the system can be obtained by equating the growth rate of variables to zero. Here, we get two equilibrium points for the proposed dynamical system, one without the biomass density of marsh plants ($M = 0$) and another point in

which all the variables are non-zero. These equilibrium points are listed as follows:

(i.) $F_0(\hat{s}, 0, \hat{S}, \hat{s_c})$,
(ii.) $F^*(s^*, M^*, S^*, s_c^*)$.

Existence of $F_0(\hat{s}, 0, \hat{S}, \hat{s_c})$
Considering the case without biomass density of marsh plant, taking $M = 0$, we have the following equations:

$$\beta(s_0 - s) - \beta_2 sS = 0, \tag{4.1}$$
$$\delta(S_0 - S) - \beta_2 sS = 0, \tag{4.2}$$
$$\theta\beta_2 sS - \theta_0 s_c = 0. \tag{4.3}$$

Solving equations (4.1) and (4.2), we get a quadratic equation in s as follows:

$$\beta\beta_2 s^2 + (\delta\beta_2 S_0 + \delta\beta - \beta\beta_2 s_0)s - \delta\beta s_0 = 0. \tag{4.4}$$

The above equation (4.4) has one positive root provided, $\delta S_0 - \beta s_0 > 0$.
Take $A_1 = \beta\beta_2$, $A_2 = \delta\beta_2 S_0 + \delta\beta - \beta\beta_2 s_0$ and $A_3 = \delta\beta s_0$.
Now,

$$\hat{s} = \frac{-A_2 + \sqrt{A_2^2 + 4A_1A_3}}{A_1}.$$

Again,

$$\hat{S} = \frac{\beta(s_0 - \hat{s})}{\beta_2\hat{s}},$$

and

$$\hat{s_c} = \frac{\theta\beta_2\hat{s}\hat{S}}{\theta_0}.$$

Existence of $F^*(s^*, M^*, S^*, s_c^*)$
In the case when $M \neq 0$, we solve the following equations:

$$\beta(s_0 - s) - \beta_1 sM - \beta_2 sS = 0, \tag{4.5}$$
$$\gamma(1 - \frac{M}{K}) - \gamma_0 + \gamma_1\beta_1 s + \gamma_2\theta_1 s_c = 0, \tag{4.6}$$
$$\delta(S_0 - S) - \beta_2 sS = 0, \tag{4.7}$$
$$\theta\beta_2 sS - \theta_0 s_c - \theta_1 s_c M = 0. \tag{4.8}$$

Simplifying, we get the following two isoclines in s and M:

$$\beta(s_0 - s) - \beta_1 sM - \beta_2 s\frac{\delta S_0}{(\beta_2 s + \delta)} = 0, \tag{4.9}$$
$$\gamma(1 - \frac{M}{K}) - \gamma_0 + \gamma_1\beta_1 s + \frac{\gamma_2\theta_1\theta\beta_2\delta s S_0}{(\theta_0 + \theta_1 M)(\beta_2 s + \delta)} = 0. \tag{4.10}$$

We notice following points from isocline (4.9),

(i.) For $M = 0$, we get quadratic equation

$$\beta\beta_2 s^2 + (\delta\beta_2 S_0 + \delta\beta - \beta\beta_2 s_0)s - \delta\beta s_0 = 0,$$

which has one positive root.
(ii.) $s \to 0$ as $M \to \infty$,
(iii.) $\frac{dM}{ds} = \frac{-(\beta s_0\delta + (\beta\beta_2 + \beta_1\beta_2 M)s^2)}{(\beta_2 s + \delta)\beta_1 s^2} < 0.$

Again, we notice following points from isocline (4.10),

(i.) we get a quadratic equation in s as follows having both negative roots for $M = 0$,
$$\gamma_1\beta_1\beta_2\theta_0 s^2 + (\gamma - \gamma_0)\theta\beta_2 + \gamma_1\beta_1\theta_0\delta + \gamma_2\theta_1\theta\beta_2\delta S_0 s + (\gamma - \gamma_0)\theta\delta = 0,$$

(ii.) $s = 0$ for $M = \dfrac{(\gamma - \gamma_0)K}{\gamma}$,

(iii.) $\dfrac{dM}{ds} = \dfrac{\{\gamma_1\beta_1(\beta_2 s + \theta)^2(\theta_0 + \theta_1 M) + \gamma_1\theta_1\theta\beta_2\delta S_0\theta\}(\theta_0 + \theta_1 M)K}{\{\gamma(\beta_2 s + \theta)(\theta_0 + \theta_1 M)^2 + \gamma_2\theta_1\theta\beta_2\delta S_0 s\theta_1\}(\beta_2 s + \theta)} > 0.$

Hence, from above it is clear that two isoclines (4.9) and (4.10) intersect each other and their intersection point (s^*, M^*) is depicted in Figure 4.1 After knowing the value of s^* and M^*, we can easily find the value of S^* and s_c^* also. The values of S^* and s_c^* are as follows:

$$S^* = \frac{\delta S_0}{(\delta + \beta_2 s^*)}, \tag{4.11}$$

$$s_c^* = \frac{\theta\beta_2 s^*\delta S_0}{(\delta + \beta_2 s^*)(\theta_0 + \theta_1 M^*)}. \tag{4.12}$$

Thus, F^* exists provided $(\delta S_0 - \beta s_0) > 0$.

Remark 4.1. *The inequality $(\delta S_0 - \beta s_0) > 0$ can be interpreted ecologically. Here, δS_0 represents the replenishment capacity of the soil system, while βs_0 denotes the effective pressure exerted by incoming salinity. For the system to reach a sustainable equilibrium, the soils ability to buffer and restore absorption sites must exceed the salinity inflow. If this condition is not met, salt accumulates uncontrollably, preventing marsh plants from surviving. In contrast, when the inequality holds, the soil functions as a stabilizing buffer, enabling the persistence of halophytes and ensuring steady desalination.*

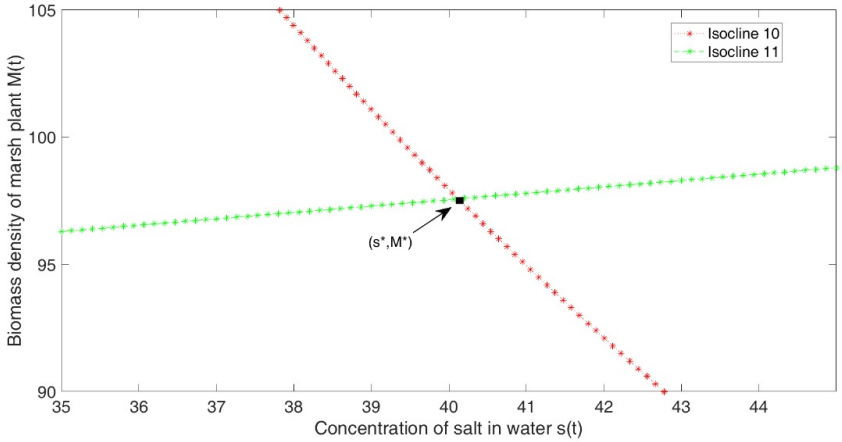

Figure* 4.1: Plot for the existence of equilibrium point F^**

5 Stability analysis

We evaluate the local and global stability of the system in this section.

Local stability of F_0

(i) To check the local stability of $F_0(\hat{s}, 0, \hat{S}, \hat{s_c})$, we find the Jacobian matrix J_0 corresponding to F_0 which is as follows:

$$J_0 = \begin{pmatrix} -(\beta + \beta_2\hat{S}) & -\beta_1\hat{s} & -\beta_2\hat{s} & 0 \\ 0 & \gamma - \gamma_0 + \gamma_1\beta_1\hat{s} + \gamma_2\theta_1\hat{s_c} & 0 & 0 \\ -\beta_2\hat{S} & 0 & -(\delta + \beta_2\hat{s}) & 0 \\ \theta\beta_2\hat{S} & -\theta_1\hat{s_c} & \theta\beta_2\hat{s} & -\theta_0 \end{pmatrix}.$$

It is noted that one of the eigen value of J_0 is $(\gamma - \gamma_0 + \gamma_1\beta_1\hat{s} + \gamma_2\theta_1\hat{s_c}) > 0$. Hence, F_0 is a saddle point and it is unstable in $M - direction$.
Now, we determine the local stability of F^* by Lyapunov's method. The condition obtained for the local stability of F^* is stated in the following theorem:

Theorem 5.1. *The Equilibrium $F^*(s^*, M^*, S^*, s_c^*)$ is locally stable provided these two conditions are satisfied:*

$$\frac{\gamma_2}{s_c^*}(\theta\beta_2 S^*)^2 < \frac{4}{9}\frac{\gamma_1}{s^*}(\theta_0 + \theta_1 M^*)(\beta + \beta_1 M^* + \beta_2 S^*), \tag{5.1}$$

$$\frac{\gamma_2}{s_c^*}(\theta\beta_2 s^*)^2(\gamma_1\beta_2 + \beta_2 S^*)^2 < \frac{4}{9}\frac{\gamma_1}{s^*}(\beta + \beta_1 M^* + \beta_2 S^*)(\delta + \beta_2 s^*)^2(\theta_0 + \theta_1 M^*). \tag{5.2}$$

Proof. To prove this theorem first, we linearize the system (2.1) about $F^*(s^*, M^*, S^*, s_c^*)$ by using the transformations

$$s = s^* + s_1, M = M^* + m, S = S^* + s_2, s_c = s_c^* + s_3, \tag{5.3}$$

where, s_1, m, s_2 and s_3 are small perturbation around F^*.
Take a positive definite function about F^*

$$V = \frac{m_1}{2}s_1^2 + \frac{m_2}{2}\frac{m^2}{M^*} + \frac{m_3}{2}s_2^2 + \frac{m_4}{2}s_3^2, \tag{5.4}$$

where, $m_1 > 0$, $m_2 > 0$, $m_3 > 0$, $m_4 > 0$ to be chosen properly.
Now, differentiating (5.4) with respect to t yields,

$$\frac{dV}{dt} = m_1 s_1\frac{ds_1}{dt} + m_2\frac{m}{M^*}\frac{dm}{dt} + m_3 s_2\frac{ds_2}{dt} + m_4 s_3\frac{ds_3}{dt}. \tag{5.5}$$

Using the model equations in (5.5) and after simplification, we get

$$\begin{aligned}\frac{dV}{dt} &= -m_1(\beta + \beta_1 M^* + \beta_2 S^*)s_1^2 - m_2\frac{\gamma m^2}{K} - m_3(\delta + \beta_2 s^*)s_2^2 \\ &\quad - m_4(\theta_0 + \theta_1 M^*)s_3^2 + (m_2\gamma_1\beta_1 - m_1\beta_1 s^*)s_1 m - (m_1\beta_2 s^* + m_3\beta_2 S^*)s_1 s_2 \\ &\quad + (m_2\gamma_2\theta_1 - m_4\theta_1 s_c^*)ms_3 + m_4\theta\beta_2 S^* s_1 s_3 + m_4\theta\beta_2 s^* s_3 s_2.\end{aligned} \tag{5.6}$$

Now, the sufficient conditions for $\frac{dV}{dt}$ come out to be negative definite are given below:

$$(m_2\gamma_1\beta_1 - m_1\beta_1 s^*)^2 < \frac{2}{3}m_1 m_2\frac{\gamma}{K}(\beta + \beta_1 M^* + \beta_2 S^*), \tag{5.7}$$

$$(m_1\beta_2 s^* + m_3\beta_2 S^*)^2 < \frac{2}{3}m_1 m_3(\beta + \beta_1 M^* + \beta_2 S^*)(\delta + \beta_2 s^*), \tag{5.8}$$

$$(m_2\gamma_2\theta_1 - m_4\theta_1 s_c^*)^2 < \frac{2}{3}m_2 m_4\frac{\gamma}{K}(\theta_0 + \theta_1 M^*), \tag{5.9}$$

$$m_4(\theta\beta_2 S^*)^2 < \frac{4}{9}m_1(\theta_0 + \theta_1 M^*)(\beta + \beta_1 M^* + \beta_2 S^*), \tag{5.10}$$

and

$$m_4(\theta\beta_2 s^*)^2 < \frac{2}{3}m_3(\theta_0 + \theta_1 M^*)(\delta + \beta_2 s^*). \tag{5.11}$$

Take $m_1 = \frac{\gamma_1}{s^*}m_2$ and $m_4 = \frac{\gamma_2}{s_c^*}m_2$ in above inequalities we get following three inequalities as follows:

$$(m_2\gamma_1\beta_2 + m_3\beta_2 S^*)^2 < \frac{2}{3}\frac{\gamma_1}{s^*}m_2 m_3(\beta + \beta_1 M^* + \beta_2 S^*)(\delta + \beta_2 s^*), \tag{5.12}$$

$$m_2\frac{\gamma_2}{s_c^*}(\theta\beta_2 s^*)^2 < \frac{2}{3}m_3(\theta_0 + \theta_1 M^*)(\delta + \beta_2 s^*), \tag{5.13}$$

$$\frac{\gamma_2}{s_c^*}(\theta\beta_2 S^*)^2 < \frac{4}{9}\frac{\gamma_1}{s^*}(\theta_0+\theta_1 M^*)(\beta+\beta_1 M^*+\beta_2 S^*). \tag{5.14}$$

Combining equations (5.12) and (5.13), then take $m_2 = m_3 = 1$, we get the required inequalities

$$\frac{\gamma_2}{s_c^*}(\theta\beta_2 S^*)^2 < \frac{4}{9}\frac{\gamma_1}{s^*}(\theta_0+\theta_1 M^*)(\beta+\beta_1 M^*+\beta_2 S^*), \tag{5.15}$$

and

$$\frac{\gamma_2}{s_c^*}(\theta\beta_2 s^*)^2(\gamma_1\beta_2+\beta_2 S^*)^2 < \frac{4}{9}\frac{\gamma_1}{s^*}(\beta+\beta_1 M^*+\beta_2 S^*)(\delta+\beta_2 s^*)^2(\theta_0+\theta_1 M^*). \tag{5.16}$$

If the above conditions (5.15) and (5.16) are satisfied then we can say system is locally stable and the interior equilibrium F^* is locally stable. □

Global stability:
To investigate global stability, we use Lyapunov's stability theory. The results regarding the global stability of the interior equilibrium F^* are stated in the following theorem:

Theorem 5.2. *Equilibrium point $F^*(s^*, M^*, S^*, s_c^*)$ is globally asymptotically stable inside the region of attraction Γ if the following two conditions hold:*

$$\theta_0\gamma_2\theta\beta_2 S_0 < \frac{4}{9}\gamma_1(\theta_0+\theta_1 M^*)(\beta+\beta_1 M^*+\beta_2 S^*), \tag{5.17}$$

and

$$(\gamma_1\beta_2+\beta_2 S_0)^2\frac{\theta_0\gamma_2\theta\beta_2 s^{*2}}{S_0} < \frac{4}{9}\gamma_1(\beta+\beta_1 M^*+\beta_2 S^*)(\delta+\beta_2 s^*)^2(\theta_0+\theta_1 M^*). \tag{5.18}$$

Proof. Take a positive definite function

$$W = \frac{k_1}{2}(s-s^*)^2 + k_2(M-M^*-M^*\ln\frac{M}{M^*}) + \frac{k_3}{2}(S-S^*)^2 + \frac{k_4}{2}(s_c-s_c^*)^2, \tag{5.19}$$

where, $k_1 > 0$, $k_2 > 0$, $k_3 > 0$, $k_4 > 0$ to be chosen properly. Now, differentiating equation (5.19) of function W with respect to t, we get

$$\dot{W} = k_1(s-s^*)\frac{ds}{dt} + k_2(1-\frac{M^*}{M})\frac{dM}{dt} + k_3(S-S^*)\frac{dS}{dt} + k_4(s_c-s_c^*)\frac{ds_c}{dt}. \tag{5.20}$$

Using model system (2.1) equations in the above equation (5.20) we get,

$$\begin{aligned}\dot{W} = &-k_1(\beta+\beta_1 M^*+\beta_2 S^*)(s-s^*)^2 - k_2\frac{\gamma}{K}(M-M^*)^2 - k_3(\delta+\beta_2 s^*)(S-S^*)^2\\ &- k_4(\theta_0+\theta_1 M^*)(s_c-s_c^*)^2 + (k_2\gamma_1\beta_1 - k_1\beta_1 s)(M-M^*)(s-s^*)\\ &- (k_1\beta_2 s + k_3\beta_2 S)(S-S^*)(s-s^*) + (k_2\gamma_2\theta_1 - k_4\theta_1 s_c)(M-M^*)(s_c-s_c^*)\\ &+ k_4\theta\beta_2 s^*(S-S^*)(s_c-s_c^*) + k_4\theta\beta_2 S(s-s^*)(s_c-s_c^*).\end{aligned} \tag{5.21}$$

$\dot{W}$ comes out to be negative definite if the following inequalities hold:

$$(k_2\gamma_1\beta_1 - k_1\beta_1 s_{max})^2 < \frac{2}{3}k_1k_2\frac{\gamma}{K}(\beta+\beta_1 M^*+\beta_2 S^*), \tag{5.22}$$

$$(k_1\beta_2 s_{max} + k_3\beta_2 S_{max})^2 < \frac{2}{3}k_1k_3(\beta+\beta_1 M^*+\beta_2 S^*)(\delta+\beta_2 s^*), \tag{5.23}$$

$$(k_2\gamma_2\theta_1 - k_4\theta_1 s_{c_{max}})^2 < \frac{2}{3}k_2k_4\frac{\gamma}{K}(\theta_0+\theta_1 M^*), \tag{5.24}$$

$$k_4(\theta\beta_2 S_{max})^2 < \frac{4}{9}k_1(\theta_0+\theta_1 M^*)(\beta+\beta_1 M^*+\beta_2 S^*), \tag{5.25}$$

and

$$k_4(\theta\beta_2 s^*)^2 < \frac{2}{3}k_3(\theta_0 + \theta_1 M^*)(\delta + \beta_2 s^*). \tag{5.26}$$

After putting maximum values in the L.H.S of the above inequalities and take $k_1 = \frac{k_2\gamma_1}{s_{max}} = \frac{k_2\gamma_1}{s_0}$ and $k_4 = \frac{k_2\gamma_2}{s_{c_{max}}} = \frac{k_2\gamma_2\theta_0}{\theta\beta_2 s_0 S_0}$, we get

$$(k_2\gamma_1\beta_2 + k_3\beta_2 S_0)^2 < \frac{2}{3}\frac{\gamma_1}{s_0}k_2k_3(\beta + \beta_1 M^* + \beta_2 S^*)(\delta + \beta_2 s^*), \tag{5.27}$$

$$k_2\frac{\gamma_2\theta_0\theta\beta_2 s^{*2}}{s_0 S_0} < \frac{2}{3}k_3(\theta_0 + \theta_1 M^*)(\delta + \beta_2 s^*), \tag{5.28}$$

$$\theta_0\gamma_2\theta\beta_2 S_0 < \frac{4}{9}\gamma_1(\theta_0 + \theta_1 M^*)(\beta + \beta_1 M^* + \beta_2 S^*). \tag{5.29}$$

Combining equation (5.27) and (5.28), then take $k_2 = k_3 = 1$, we get the required inequalities.

$$\theta_0\gamma_2\theta\beta_2 S_0 < \frac{4}{9}\gamma_1(\theta_0 + \theta_1 M^*)(\beta + \beta_1 M^* + \beta_2 S^*), \tag{5.30}$$

and

$$(\gamma_1\beta_2 + \beta_2 S_0)^2\frac{\theta_0\gamma_2\theta\beta_2 s^{*2}}{S_0} < \frac{4}{9}\gamma_1(\beta + \beta_1 M^* + \beta_2 S^*)(\delta + \beta_2 s^*)^2(\theta_0 + \theta_1 M^*). \tag{5.31}$$

If the inequalities (5.30) and (5.31) holds then $\frac{dW}{dt}$ is negative definite. Hence, the interior equilibrium point F^* is globally asymptotically stable inside Ω. This is the complete proof of the Theorem 5.2. □

6 Numerical Simulation

To examine the validity of analytic solutions and the feasibility of the model system (2.1), we conduct the simulation using *MATLAB* for the parameter values described in the Table 6.1. The equilibrium point F^* is obtained numerically as:
$s^* = 40.12$, $M^* = 97.5748896$, $S^* = 44.102073$, $s_c^* = 89.7479$.
In this section, plots showing the effect of different values of parameters on the state variables are illustrated and we also investigate the global stability of the system.
We see that the first three Figures 6.1- 6.3 depict the effect of variation of γ_1, β_1 and β_2 on the concentration of salt in water, respectively. It is observed from Figure 6.1 that as we increase the value of γ_1 there is a decrease in the concentration of salt in the water due to an increase in biomass density of marsh plants. In Figures. 6.2 - 6.3, we observe that the concentration of salt in water decreases with the increase in values of both β_1 and β_2. Now, from Figure 6.4, we conclude that the biomass density of marsh plants increases with the value of γ_1. It is noted from Figures 6.5- 6.6 that the growth of γ_1 and β_1 affects positively, the concentration of soil. From Figure 6.7 we analyze that the concentration of soil decreases with the increase in value of β_2. In Figures 6.8- 6.11, we see the plots showing the effect of parameters on the concentration of salt in the soil. It is noticed from Figures 6.8 and 6.10 that the concentration of salt in soil decreases with the increase in values of γ_1, β_1 and θ_1 parameters but from Figures 6.9 and 6.11, we conclude that the concentration of salt in the soil increases with an increase in parameters β_2 and θ. Now, Figures 6.12- 6.14 show the global stability of the equilibrium F^*. Figures 6.12 and 6.13 depict the two-dimensional global stability plots, here all the solution paths starting anywhere inside the region of attraction converge towards the equilibrium point F^* in $s-M$-plane and $s-S$-plane respectively. Also, in Figure 6.14 all the solution trajectories converge to the equilibrium point showing three-dimensional global stability in $s-M-S$-space. In Figure 6.15, surface plots illustrate the concentration of salt in water and biomass density of marsh plants with respect to β_1 i.e. depletion rate coefficient of concentration of salt in water and γ i.e. intrinsic growth rate of biomass density of marsh plant simultaneously. We observe from these plots that as the rate β_1 and γ increase, concentration of salt in water decreases and the biomass density of marsh plant increases.

***Table* 6.1:** *Description table for various parameters and variables*

Description of parameter	Symbol	Units and values
Growth rate coefficient of concentration of salt in water	β	0.1 per day
Equilibrium concentration of salt in water	s_0	1000 g/L
depletion rate coefficient for salt using marsh plants	β_1	0.02 square m per g per day
depletion rate coefficient for salt due to soil salination	β_2	0.01 L per kg per day
Intrinsic growth rate of biomass density of marsh plants	γ	0.8 per day
Natural depletion in biomass density of marsh plants	γ_0	0.1 per day
Carrying capacity of the marsh plants biomass density	K	100 g per square m
Proportionality constant	γ_1	0.1 L per square m
Proportionality constant	γ_2	0.2 m
Growth rate coefficient of concentration of soil	δ	3 per day
Equilibrium concentration of soil	S_0	50 kg/L
Proportionality constant for growth of concentration of salt in soil	θ	0.01 unit less quantity=0.001
Natural depletion in concentration of salt in soil	θ_0	0.00002 per day
Depletion rate coefficient due to marsh plants in concentration of salt in soil	θ_1	0.00002 square m per g per day
Time	t	day
Concentration of salt in water	$s(t)$	g/L
Biomass density of marsh plants	$M(t)$	g per square m
Concentration of soil	$S(t)$	kg/L
Concentration of salt in soil	$s_c(t)$	mg/L

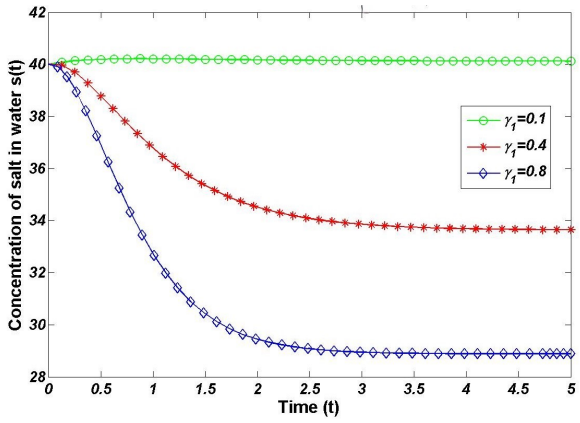

***Figure* 6.1:** *Variation in concentration of salt in water $s(t)$ for distinct values of γ_1.*

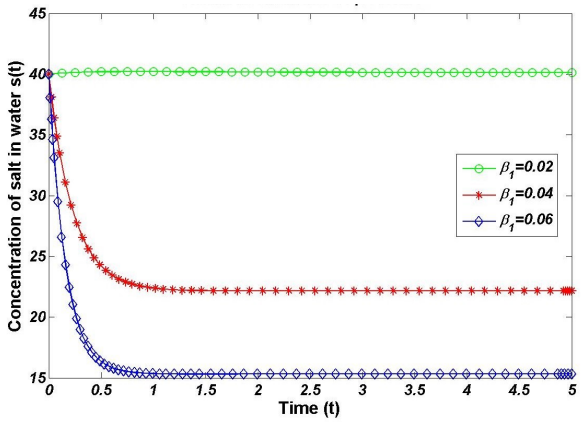

***Figure* 6.2:** *Variation in concentration of salt in water $s(t)$ for distinct values of β_1.*

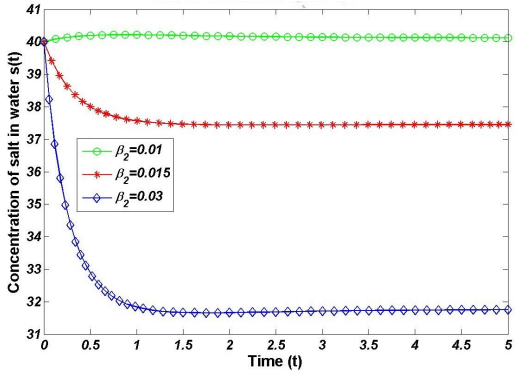

***Figure* 6.3:** *Variation in concentration of salt in water $s(t)$ for distinct values of β_2.*

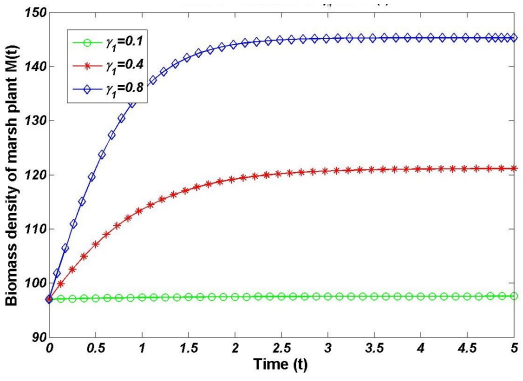

***Figure* 6.4:** *Variation in biomass density of marsh plants $M(t)$ for distinct values of γ_1.*

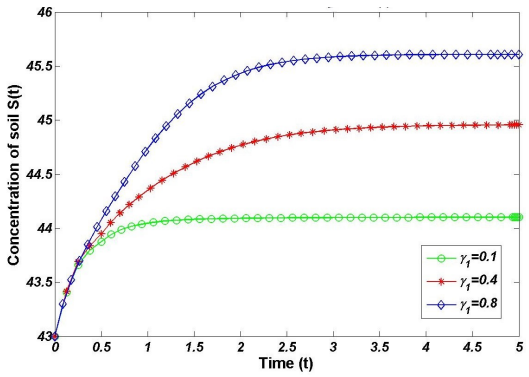

***Figure* 6.5:** *Variation in concentration of soil $S(t)$ for distinct values of γ_1.*

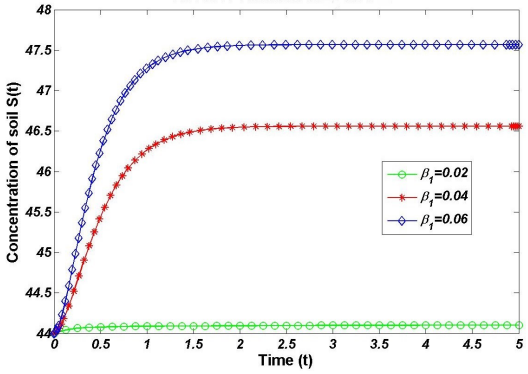

***Figure* 6.6:** *Variation in concentration of soil $S(t)$ for distinct values of β_1.*

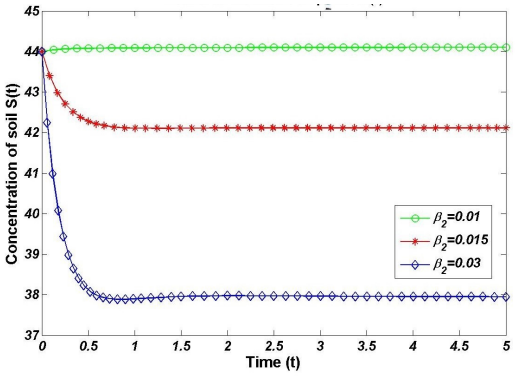

***Figure* 6.7:** *Variation in concentration of soil $S(t)$ for distinct values of β_2.*

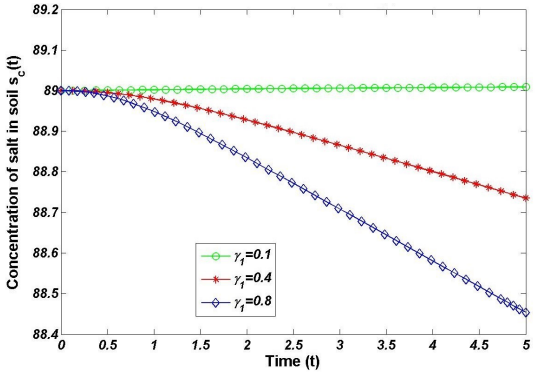

***Figure* 6.8:** *Variation in concentration of salt in soil $s_c(t)$ for distinct values of γ_1.*

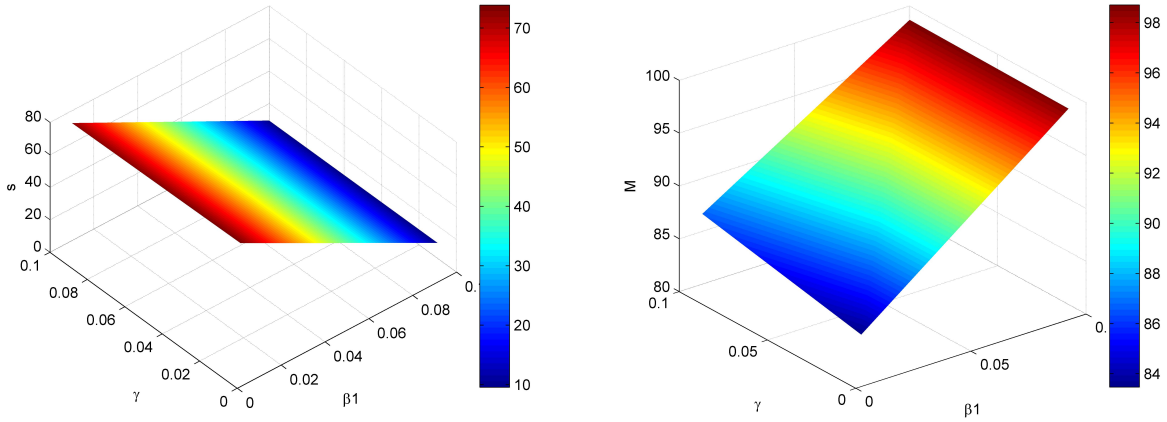

(a) ***(b)***

***Figure* 6.15:** *Surface plots of (a) concentration of salt in water, (b) biomass density of marsh plants with respect to β_1, γ at time t=5.*

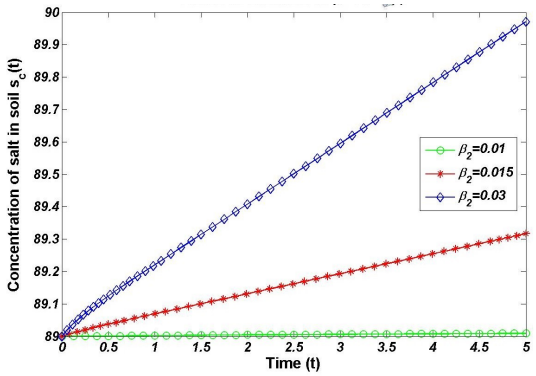

Figure* 6.9: Variation in concentration of salt in soil $s_c(t)$ for distinct values of β_2.*

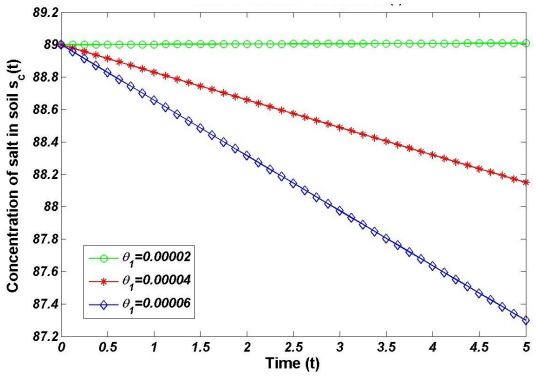

Figure* 6.10: Variation in concentration of salt in soil $s_c(t)$ for distinct values of θ_1.*

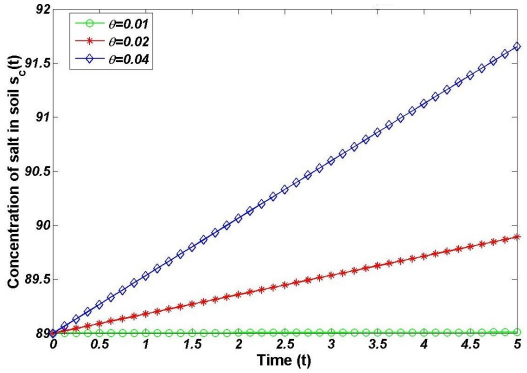

Figure* 6.11: Variation in concentration of salt in soil $s_c(t)$ for distinct values of θ.*

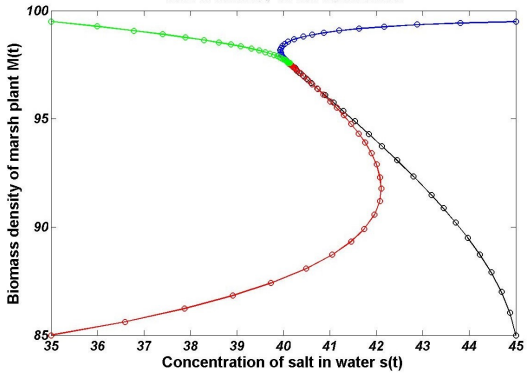

Figure* 6.12: Global stability of interior equilibrium F^* in $s-M$-plane.*

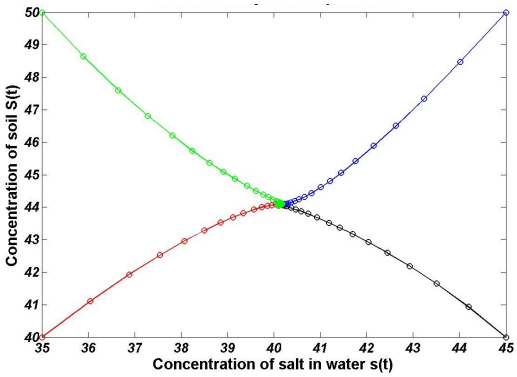

Figure* 6.13: Global stability of interior equilibrium F^* in $s-S$-plane.*

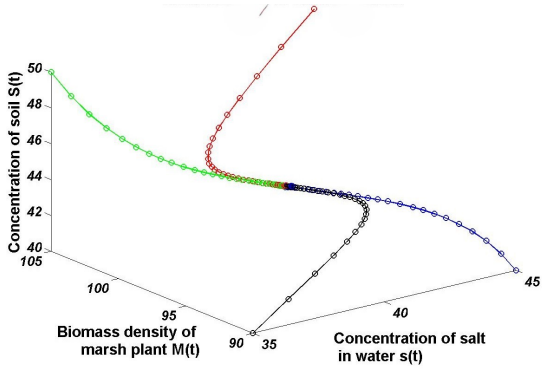

Figure* 6.14: Global stability of interior equilibrium F^* in $s-M-S$-space.*

7 Sensitivity analysis

In this section, basic differential sensitivity analysis considering Bortz and Nelson (2004) is carried out to investigate out how sensitive the dependent variables s, M, S, s_c of system (2.1) are corresponding to change in prompting parameters γ_1, β_1, β_2. Considering the sensitivity function $Z_v(t,v) = \dfrac{\partial Z(t,v)}{\partial v}$, we can calculate semi-relative sensitivity solutions (i.e. $vZ_v(t,v)$), where Z is the state variable and v is the parameter. Here, these semi-relative sensitivity solutions represent the effect on the state variables as we double prompting parameters.

Now, the semi- relative sensitivity solution for the variables with respect to parameter γ_1 is as follows:

$$\left.\begin{aligned}
\dot{s_{\gamma_1}}(t,\gamma_1) &= -\beta s_{\gamma_1}(t,\gamma_1) - \beta_1 s_{\gamma_1}(t,\gamma_1)M(t,\gamma_1) - \beta_1 s(t,\gamma_1)M_{\gamma_1}(t,\gamma_1)\\
&\quad - \beta_2 s_{\gamma_1}(t,\gamma_1)S(t,\gamma_1) - \beta_2 s(t,\gamma_1)S_{\gamma_1}(t,\gamma_1)\\
\dot{M_{\gamma_1}}(t,\gamma_1) &= \gamma\left(M_{\gamma_1}(t,\gamma_1) - 2\frac{M(t,\gamma_1)M_{\gamma_1}(t,\gamma_1)}{K}\right) - \gamma_0 M_{\gamma_1}(t,\gamma_1)\\
&\quad + \beta_1 s(t,\gamma_1)M(t,\gamma_1) + \gamma_1\beta_1 s_{\gamma_1}(t,\gamma_1)M(t,\gamma_1) + \gamma_1\beta_1 s(t,\gamma_1)M_{\gamma_1}(t,\gamma_1)\\
&\quad + \gamma_2\theta_1 s_{c_{\gamma_1}}(t,\gamma_1)M(t,\gamma_1) + \gamma_2\theta_1 s_c(t,\gamma_1)M_{\gamma_1}(t,\gamma_1)\\
\dot{S_{\gamma_1}}(t,\gamma_1) &= -\delta S_{\gamma_1}(t,\gamma_1) - \beta_2 s_{\gamma_1}S(t,\gamma_1) - \beta_2 s(t,\gamma_1)S_{\gamma_1}(t,\gamma_1)\\
\dot{s_{c_{\gamma_1}}}(t,\gamma_1) &= \theta\beta_2 s_{\gamma_1}(t,\gamma_1)S(t,\gamma_1) + \theta\beta_2 s(t,\gamma_1)S_{\gamma_1}(t,\gamma_1)\\
&\quad - \theta_0 s_{c_{\gamma_1}}(t,\gamma_1) - \theta_1 s_{c_{\gamma_1}}(t,\gamma_1)M(t,\gamma_1) - \theta_1 s_c(t,\gamma_1)M_{\gamma_1}(t,\gamma_1).
\end{aligned}\right\} \tag{7.1}$$

Similarly, we can find the semi-relative sensitive solution with respect to key parameters.

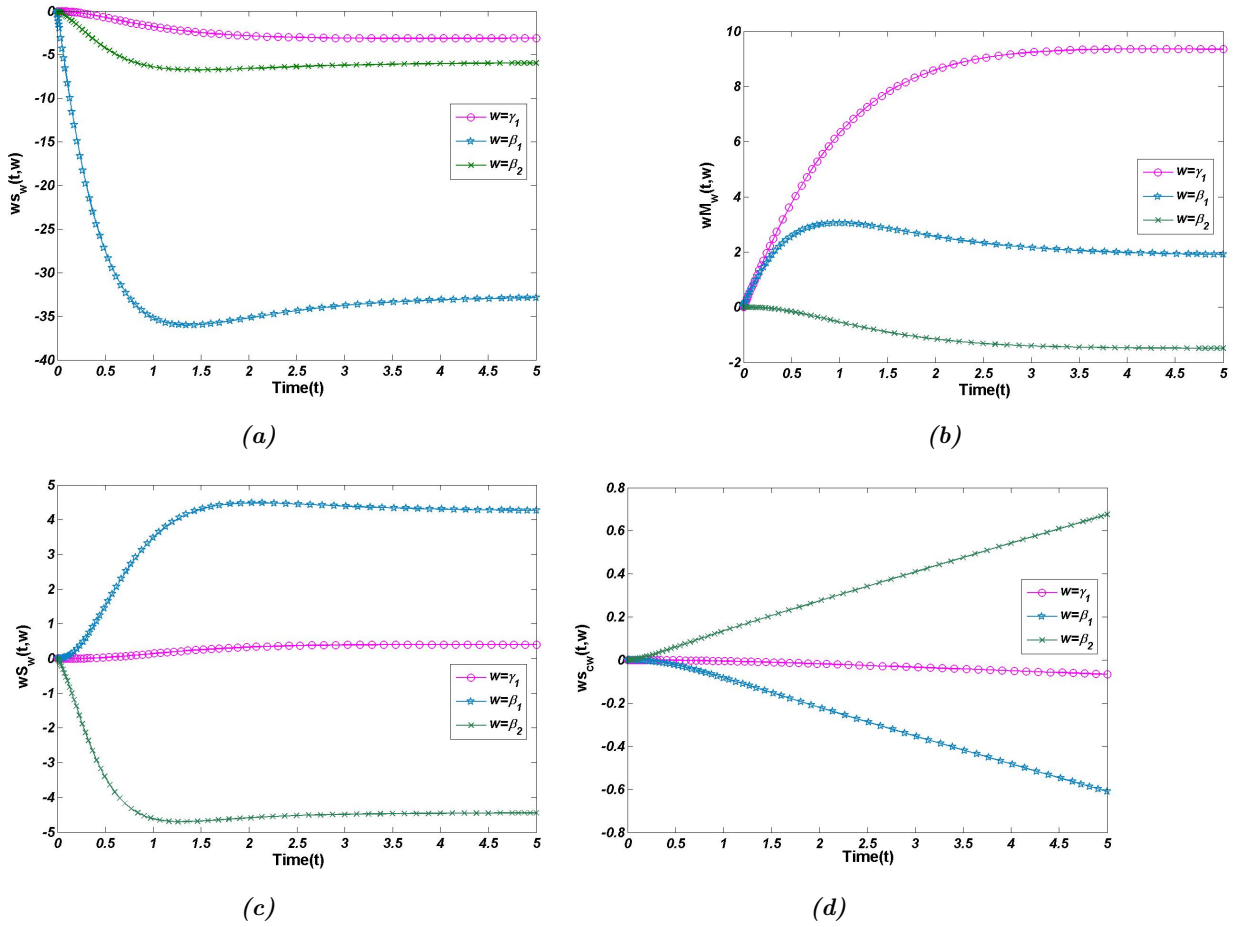

Figure 7.1: *Plots of semi-relative basic differential sensitivity taking parameters γ_1, β_1, β_2 for different state variables*

Figure 7.1 contains the plots of semi-relative sensitivity of state variables s, M, S, s_c with respect to the key parameters γ_1, β_1, β_2. Here, in these plots, we observe the behaviour of variables corresponding to the doubling of parameters. From Figure 7.1a, we see that doubling of all parameters γ_1, β_1, β_2 lowering the concentration of salt $s(t)$ in water, because these parameters help reduce the concentration of salt in the reservoir using marsh plants and soil salinization in time t= 5 days. Again, from Figure 7.1b we conclude that doubling of two parameters γ_1 and β_1 has a positive impact on the growth of marsh plants because both the parameters γ_1 and β_1 are used to extract salt from water by marsh plant and salt exhibits the growth of marsh plants. But, the parameter β_2 has no impact on the growth of biomass of marsh plants $M(t)$. It is noticed from Figure 7.1c that doubling of parameter β_1 has a positive impact on the concentration of soil in the reservoir, it is increased by 4.265 kg/L in t= 5 days. However, the doubling of parameter γ_1 has no effect and parameter β_2 decrease the concentration of soil in the reservoir. From Figure 7.1d, we observe that doubling of β_2 has a positive impact on the concentration of salt in the soil and it is increased by 0.6761 mg/L in 5 days while the other parameter γ_1 has no effect and β_1 affects negatively the concentration of salt in the soil. Table 7.1 shows the results of the plots of semi-relative basic differential sensitivity.

Table* 7.1*: *Semi-relative sensitive analysis*

Parameter	$s(t)$	$M(t)$	$S(t)$	$s_c(t)$
γ_1	negative effect	positive effect	no effect	no effect
β_1	negative effect	positive effect	positive effect	negative effect
β_2	negative effect	negative effect	negative effect	positive effect

The sensitivity analysis highlights the parameters most influential in regulating the desalination process. For instance, parameters γ_1 and β_1, which govern salt uptake by marsh plants, strongly influence both plant biomass and salt removal from water. This is consistent with the ecological observation that halophytes utilize salt as a resource for growth up to a threshold. On the other hand, β_2, which measures salt absorption through soil buffering, primarily affects soil salinity but has little direct impact on plant biomass in the present model. These outcomes underscore the different ecological roles of marsh plants and soil: the former act as active salt consumers, while the latter serve as a buffering medium that stabilizes the system indirectly.

8 Results and Conclusion

The blue planet Earth is almost covered with water but fresh-water resources availability is rare due to mismanagement and environmental changes. This perilous condition of freshwater crisis due to increasing population, water pollution, and urbanization can be curbed by appropriate water management methods like reusing and purifying wastewater. Desalination of saline water is considered as an enticing way to mitigate the water stress. In the current predicament, our interest is to adopt a cheaper and more economically profitable way for desalination like the use of halophytes (marsh plants) because these can resist high salinity medium and absorb salt from saline water. Contemplating the above fact, we proposed and analyzed a non-linear mathematical model with an interoperability of four variables namely, the concentration of salt in water $s(t)$, the biomass density of marsh plants $M(t)$, the concentration of soil in the reservoir $S(t)$, the concentration of salt in soil due to soil salinization $s_c(t)$. In this paper, we attempt to desalinate saline water within a reservoir containing marsh plants and soil, both marsh plants and soil soak up salt from the water and this leads to a reduction of salt in the water. Here, we see in this process both marsh plants and soil work as predators and saline water as prey, simultaneously we see that salty soil is also prey for marsh plants.

The present model makes simplifying but ecologically justified assumptions. Marsh plants are treated as halophytes, a group known to respond positively to salinity within certain limits, which explains the growth-promoting role of salt in the model. Soil dynamics are represented in terms of effective buffering capacity, emphasizing its role as a stabilizing reservoir rather than as a nutrient source. While the model does not explicitly include inhibitory effects of extreme salinity or nutrientplant feedbacks, it successfully captures the qualitative interplay between water salinity, plant biomass, and soil buffering. This provides a baseline mathematical framework for understanding halophyte-assisted desalination in reservoirs.

In this modelling study, it is assumed that marsh plants grow logistically, and a high saline medium enhances their growth and carrying capacity. Also, soil salination occurs in this process and is accountable for the abatement in the concentration of salt in water. The mathematical analysis shows that as the density of marsh plants increases concentration of salt in water as well as in soil decreases. In this paper, the condition